Proc. Int. Symposium on Advances in Neutron Scattering Research, Tokai, 2000
J. Phys. Soc. Jpn. **70** (2001) Suppl. A pp. 76–78

# Interrelation between Orbital Stability and Charge-Ordering Transition in Doped Manganites

Akihiko MACHIDA[1], Yutaka MORITOMO[2], Kenji OHOYAMA[3] and Arao NAKAMURA[2]

[1] *Department of Crystalline Materials Science, Nagoya University, Nagoya 464-8603, Japan*
[2] *Center for Integrated Research in Science and Engineering, Nagoya University, Nagoya 464-8603, Japan*
[3] *Institute for Materials Research, Tohoku University, Sendai 980-8577, Japan*

Lattice effects on the charge/orbital-ordering transition of doped manganites, $R_{2/3}Ca_{1/3}MnO_3$ ($R$=La, Pr, Nd, $Nd_{1/2}Tb_{1/2}$, and Tb), have been investigated changing the averaged ionic radius $\langle r_R \rangle$ of the rare-earth ions (chemical pressure). We have performed neutron powder diffraction experiments at room temperature and have found a close correlation between the charge-ordering transition and the shape of the $MnO_6$ octahedra. In comparison with the half-doped manganites, interrelation between the orbital stability and the charge/orbital-ordering transition is discussed.

KEYWORDS: perovskite-type doped manganites, neutron powder diffraction, orbital stability

## §1. Introduction

Perovskite-type doped manganites $R_{1-x}A_xMnO_3$, where $R$ and $A$ are trivalent rare-earth and divalent alkaline-earth ions, respectively, have three-dimensional networks of the $MnO_6$ octahedra. By changing the averaged ionic radius $\langle r_A \rangle$ of the perovskite $A$-site, the Mn–O–Mn angle, or the transfer integral $t$ between the neighboring Mn sites, is modified (*chemical pressure*). It is well known that the Curie temperature $T_C$ is suppressed with decrease of the $\langle r_A \rangle$-value. Radaelli *et al.*[1] have performed a systematic neutron structural analysis at a fixed $x$ (= 0.3), and have observed a close correlation between the $t$-value and $T_C$. Similar to the case of the Curie temperature, the chemical pressure effect on the critical temperature $T_{CO}$ for the charge-ordering transition have been regarded as control of $t$. In the doped manganites, it is established that the charge-ordering transition accompanies $d_{3x^2-r^2}/d_{3y^2-r^2}$ orbital alternation,[2] and that the shape of $MnO_6$ octahedra relates to the stability of the Mn $e_g$-orbitals.[3] Recently, Machida *et al.*[4] have reexamined the interrelation between the structural parameters and $T_{CO}$ of the half-doped ($x$=1/2) manganites, $R_{1/2}A_{1/2}MnO_3$. They have found a close correlation between $T_{CO}$ and the shape of the $MnO_6$ octahedra: $T_{CO}$ is governed by the orbital stability.

To confirm that the above-mentioned trend is applicable to the other hole concentration, we have extended our research to the $x = 1/3$ system. We found a close correlation between the orbital stability, which was estimated from the shape of the $MnO_6$ octahedra in an electrostatic manner, and the charge-ordering transition. This result indicates that the orbital stability is an important factor for the charge-/orbital-ordering transition of doped manganites.

## §2. Experimental

A series of ceramics compounds, $R_{2/3}Ca_{1/3}MnO_3$ ($R$=La, Pr, Nd, $Nd_{1/2}Tb_{1/2}$ and Tb), was synthesized by solid state reaction in an air atmosphere. Neutron powder diffraction measurements were performed with the Kinken powder diffractometer for high efficiency and high resolution measurements (HERMES)[5] installed at the JRR-3M reactor at the Japan Atomic Energy Research Institute, Tokai, Japan. Neutrons with wavelength 1.8196 Å were obtained by the 331 reflection of the Ge monochromator, and 12′-B-Sample-22′ collimation. We have analyzed the neutron powder patterns at room temperature with RIETAN-97$\beta$ program,[6] and

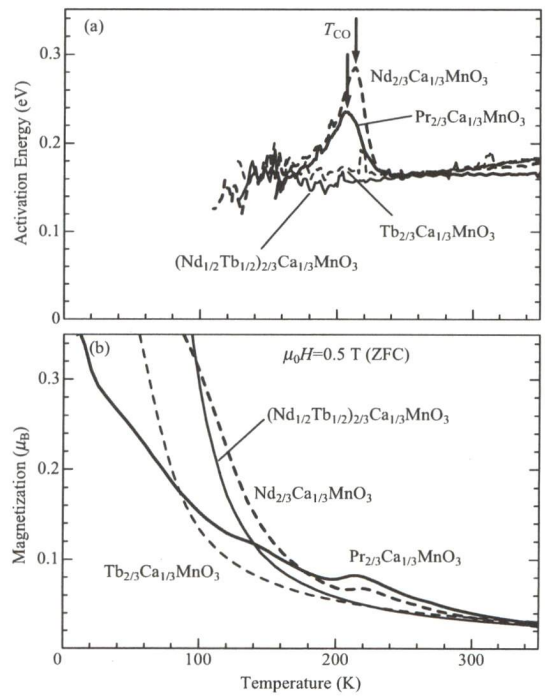


Fig. 1. Temperature variation of (a) activation energy $E_{ac}$ [= $d(\ln \rho)/d(1/T)$; $\rho$ is resistivity] and (b) magnetization $M$ for $R_{2/3}Ca_{1/3}MnO_3$. $M$ was measured after cooling down to 10 K in the zero field (ZFC). Downward arrows indicate the critical temperatures $T_{CO}$ for the charge-ordering transition.

Table I. Lattice constants and atomic positions for $R_{2/3}Ca_{1/3}MnO_3$ determined from neutron powder profiles at room temperature. $g$ means oxygen occupancy determined by Rietveld analysis. The crystal symmetry is orthorhombic ($Pbnm$; $Z$=4). The atomic sites are $R$/Ca $4c[x, y, \frac{1}{4}]$, Mn $4b[\frac{1}{2}, 0, 0]$, O(1) $4c[x, y, \frac{1}{4}]$, O(2) $8d[x, y, z]$. $T_{CO}$ and $T_C$ are the charge-ordering and Curie temperatures, respectively. We also listed the Mn–O bondlength, $d_x$, $d_y$, and $d_z$.

| | $a$ (Å) | $b$ (Å) | $c$ (Å) | $R_{wp}$ (%) | $R_I$ (%) | $T_{CO}$ (K) | $T_C$ (K) | $g$ |
|---|---|---|---|---|---|---|---|---|
| $La_{2/3}Ca_{1/3}MnO_3$ | 5.4737(3) | 5.4595(4) | 7.7124(4) | 3.56 | 2.02 | — | 260 | 1.015(5) |
| $Pr_{2/3}Ca_{1/3}MnO_3$ | 5.4277(3) | 5.4532(2) | 7.6687(4) | 4.28 | 2.69 | 207 | — | 1.018(5) |
| $Nd_{2/3}Ca_{1/3}MnO_3$ | 5.4097(3) | 5.4625(2) | 7.6493(4) | 4.79 | 2.08 | 213 | — | 0.999(5) |
| $(Nd_{1/2}Tb_{1/2})_{2/3}Ca_{1/3}MnO_3$ | 5.3659(3) | 5.5042(2) | 7.5640(4) | 4.20 | 1.93 | — | — | 0.980(6) |
| $Tb_{2/3}Ca_{1/3}MnO_3$ | 5.3249(2) | 5.5519(1) | 7.4776(2) | 4.53 | 2.00 | — | — | 0.995(5) |

| $R$/Ca | | O(1) | | O(2) | | | | | |
|---|---|---|---|---|---|---|---|---|---|
| $x$ | $y$ | $x$ | $y$ | $x$ | $y$ | $z$ | $d_x$ (Å) | $d_y$ (Å) | $d_z$ (Å) |
| 0.003(1) | −0.0205(8) | 0.937(1) | 0.506(1) | 0.2748(9) | 0.7227(9) | 0.0329(5) | 1.951(7) | 1.969(7) | 1.959(1) |
| 0.009(2) | −0.0335(9) | 0.931(1) | 0.5118(8) | 0.2857(6) | 0.7132(5) | 0.0377(4) | 1.959(5) | 1.971(5) | 1.954(1) |
| 0.0075(9) | −0.0388(6) | 0.931(1) | 0.5141(7) | 0.2882(6) | 0.7090(5) | 0.0398(4) | 1.956(4) | 1.983(4) | 1.950(1) |
| 0.0116(7) | −0.0494(5) | 0.9183(7) | 0.5188(7) | 0.2915(5) | 0.7046(5) | 0.0420(3) | 1.956(4) | 1.995(4) | 1.943(1) |
| 0.0121(5) | −0.0603(4) | 0.9116(5) | 0.5233(5) | 0.2965(4) | 0.6992(4) | 0.0457(3) | 1.958(3) | 2.020(3) | 1.9322(8) |

have found that the investigated compounds were single phase without detectable impurities. The crystal symmetry is orthorhombic ($Pbnm$; $Z$=4). Thus obtained lattice parameters, as well as oxygen occupancy, at room temperature are listed in Table I.

In order to determine $T_{CO}$ and $T_C$, we have measured temperature variation of resistivity $\rho$ and magnetization $M$. Figure 1 shows temperature variation of (a) activation energy $E_{ac}$ [$\equiv d(\ln\rho)/d(1/T)$, where $\rho$ is resistivity] and (b) magnetization $M$ of $R_{2/3}Ca_{1/3}MnO_3$. The $E_{ac}-T$ curve of $Pr_{2/3}Ca_{1/3}MnO_3$ (thick solid curve) and $Nd_{2/3}Ca_{1/3}MnO_3$ (thick dashed curve) have a peak due to the charge-ordering transition. $T_{CO}$ was defined as the maximal point (downward arrow) of the $E_{ac}-T$ curve. On the other hand, in $(Nd_{1/2}Tb_{1/2})_{2/3}Ca_{1/3}MnO_3$ (thin solid curve) and $Tb_{2/3}Ca_{1/3}MnO_3$ (thin dashed curve), the $E_{ac}-T$ curves have no peaks, indicating absence of the charge-ordering transition. $M$ was measured under a field of $\mu_0 H$=0.5 T after cooling down to 10 K in the zero field (ZFC). In $La_{2/3}Ca_{1/3}MnO_3$, ferromagnetic transition was observed at $\approx$ 260 K (not shown). $T_C$ was determined from an inflection point of the $M-T$ curve. Thus determined $T_{CO}$ and $T_C$ are also listed in Table I.

## §3. Results and Discussion

In Fig. 2, thus obtained (a) $T_C$ and (b) $T_{CO}$ are plotted against the averaged Mn–O–Mn angles $\langle\Theta\rangle$ calculated from the structural parameters (see Table I). Open and closed circles represent the $x$=1/3 and $x$=1/2[4] systems, respectively. One may observe a close correlation between $\langle\Theta\rangle$ and $T_C$ in Fig. 2(a): with decrease of $\langle\Theta\rangle$, $T_C$ decreases from $\sim$ 360 K and then disappears around $\langle\Theta\rangle \sim 160°$. Such a close correlation should be ascribed to the geometrically suppressed $t$ [$t \propto \sin(\Theta/2)$]. On the other hand, there appears no correlation between $T_{CO}$ and $\langle\Theta\rangle$ [see Fig. 2(b)]; in spite of smaller $\langle\Theta\rangle$-value, the charge-ordering transition is absent in $(Nd_{1/2}Tb_{1/2})_{2/3}Ca_{1/3}MnO_3$ and $Tb_{2/3}Ca_{1/3}MnO_3$. Recently, we have investigated the lattice effect on the charge-ordering transition of $R_{1/2}A_{1/2}MnO_3$, and found that the chemical pressure effect on the charge-ordering

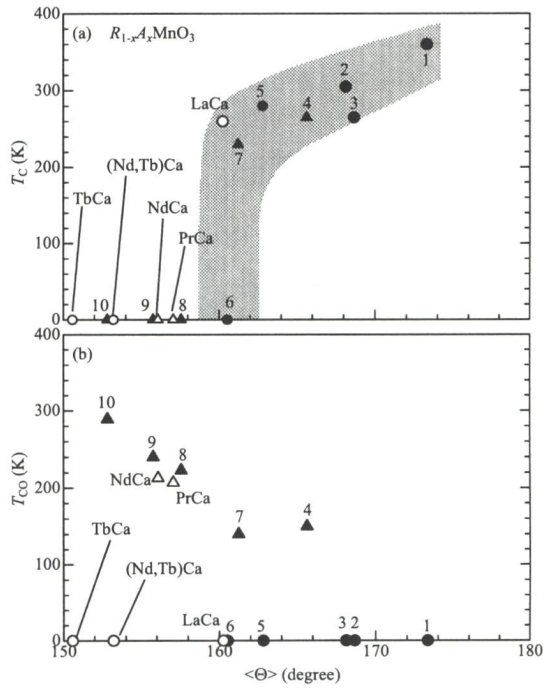


Fig. 2. (a) Curie Temperature and (b) critical temperature $T_{CO}$ for the charge-ordering transition of $R_{1-x}A_xMnO_3$ ($x$=1/2 and 1/3) against the averaged Mn–O–Mn angle $\langle\Theta\rangle$ calculated from the structural parameters. Open and closed symbols represents the $x$=1/3 and $x$=1/2 systems, respectively. Triangle (circle) presents that the sample (does not) show the charge-ordering transition. Hatching is a guide to the eye. Number indicates that the data were cited from Ref. 2: 1. $La_{1/2}Sr_{1/2}MnO_3$, 2. $(La_{1/2}Nd_{1/2})_{1/2}Sr_{1/2}MnO_3$, 3. $Pr_{1/2}Sr_{1/2}MnO_3$, 4. $Nd_{1/2}Sr_{1/2}MnO_3$, 5. $(Nd_{1/2}Tb_{1/2})_{1/2}Sr_{1/2}MnO_3$, 6. $Tb_{1/2}Sr_{1/2}MnO_3$, 7. $La_{1/2}Ca_{1/2}MnO_3$, 8. $Nd_{1/2}Ca_{1/2}MnO_3$, 9. $(Nd_{1/2}Tb_{1/2})_{1/2}Ca_{1/2}MnO_3$, and 10. $Tb_{1/2}Ca_{1/2}MnO_3$.

transition has an aspect of orbital control, besides the control of $t$.[4] In other words, the stability of the $e_g$-orbitals is an important factor for the charge-ordering transition. Note that the $d_{3x^2-r^2}/d_{3y^2-r^2}$ orbital alternation is established in the charge-ordered phase.[2]

To estimate the relative stability of the respective $e_g$-

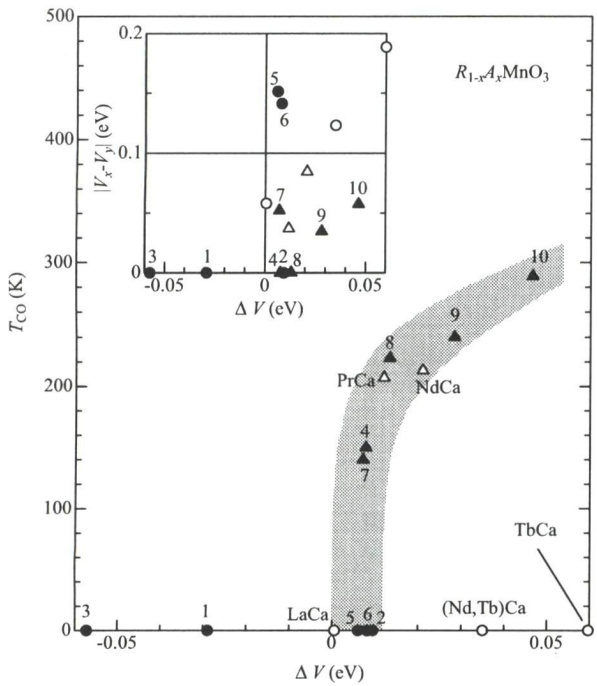


Fig. 3. Critical temperature $T_{CO}$ of the charge-ordering transition for $R_{1-x}A_xMnO_3$ ($x$=1/2 and 1/3) against the relative orbital stability $\Delta V$ (see text). Open and closed symbols represents the $x$=1/3 and $x$=1/2 systems, respectively. Triangle (circle) presents that the sample (does not) show the charge-ordering transition. Hatching is a guide to the eye. Inset shows mapping of the data points into the $\Delta V$–$|V_x - V_y|$ plane. Number indicates that the data were cited from Ref. 2: 1. $La_{1/2}Sr_{1/2}MnO_3$, 2. $(La_{1/2}Nd_{1/2})_{1/2}Sr_{1/2}MnO_3$, 3. $Pr_{1/2}Sr_{1/2}MnO_3$, 4. $Nd_{1/2}Sr_{1/2}MnO_3$, 5. $(Nd_{1/2}Tb_{1/2})_{1/2}Sr_{1/2}MnO_3$, 6. $Tb_{1/2}Sr_{1/2}MnO_3$, 7. $La_{1/2}Ca_{1/2}MnO_3$, 8. $Nd_{1/2}Ca_{1/2}MnO_3$, 9. $(Nd_{1/2}Tb_{1/2})_{1/2}Ca_{1/2}MnO_3$, and 10. $Tb_{1/2}Ca_{1/2}MnO_3$.

orbitals, that is, $d_{3x^2-r^2}$, $d_{3y^2-r^2}$ and $d_{3z^2-r^2}$, we have calculated the electrostatic potentials, $V_x$, $V_y$, and $V_z$, based on the structural data shown in Table I. For the $d_{3x^2-r^2}$ orbital, we calculated the potential $V_x$ acting on the two $e/2$-charges located on the Mn–O bonds along $x$-direction:,

$$V_x = 2[V(d_x - r_d) + V(d_x + r_d) + 2V(\sqrt{d_y^2 + r_d^2}) + 2V(\sqrt{d_z^2 + r_d^2})], \quad (3.1)$$

where $V(r)$ is the electrostatic potential between $O^{2-}$ and the $e/2$-charge. Similarly, we calculated the potentials, $V_y$ and $V_z$, for the $d_{3y^2-r^2}$ and $d_{3z^2-r^2}$ orbitals as

$$V_y = 2[V(d_y - r_d) + V(d_y + r_d) + 2V(\sqrt{d_z^2 + r_d^2}) + 2V(\sqrt{d_x^2 + r_d^2})], \quad (3.2)$$

and

$$V_z = 2[V(d_z - r_d) + V(d_z + r_d) + 2V(\sqrt{d_x^2 + r_d^2}) + 2V(\sqrt{d_y^2 + r_d^2})]. \quad (3.3)$$

Here, $d_x$, $d_y$, and $d_z$ indicate the Mn–O bondlength and $r_d$ (=0.42 Å) is the radius where the radial charge density of the Mn $3d$ orbital becomes maximum. The larger $V_i$ are, the more stable the corresponding orbital becomes. The stability of the $d_{3x^2-r^2}/d_{3y^2-r^2}$ orbital alternation can be estimated from the difference of the potentials $\Delta V$:

$$\Delta V = (V_x + V_y)/2 - \langle V \rangle. \quad (3.4)$$

Here, $\langle V \rangle$ [$\equiv (V_x + V_y + V_z)/3$] is the averaged value.

In Fig. 3, we plotted $T_{CO}$ against $\Delta V$. Triangle shows the charge-ordering transition, while circle does not show it. If one sees the phase diagram from left to right (the stability of the $d_{3x^2-r^2}/d_{3y^2-r^2}$ orbital alternation increases.), the COI state appears and $T_{CO}$ increases. However, there are exceptions on this trend (see open circles at $\Delta V$ = 0.034 and 0.06 in Fig. 3), suggesting that an extra factor is needed for the charge-ordering transition. We mapped in the inset of Fig. 3 the data points against $\Delta V$ and $|V_x - V_y|$, the latter of which represents the relative stability between the $d_{3x^2-r^2}$ and $d_{3y^2-r^2}$ orbitals. The triangles (the samples that show the charge-ordering transition) gather in the lower right corner. This suggests that the large $\Delta V$ as well as the small $|V_x - V_y|$ are necessary conditions for the charge-ordering transition. Intuitively speaking, the negative Jahn-Teller distortion, that is, two long and one short bonds, is needed for the charge-ordering transition.

## §4. Summary

We have investigated the interrelation between the charge-ordering transition and the orbital stability of doped manganites by means of neutron structural analysis. We have found that the chemical pressure effect on the charge-ordering transition has an aspect of orbital control for not only in the half-doped ($x$ = 1/2) system but also in the $x$=1/3 system.

## Acknowledgements

This work was supported by a Grant-In-Aid for Scientific Research from the Ministry of Education, Science, Sports and Culture.

1) P. G. Radaelli, G. Iannone, M. Marezio, H.-Y. Hwang, S.-W. Cheong, J. D. Jorgensen and D. N. Argyriou: Phys. Rev. B **56** (1997) 8265.
2) Y. Murakami, H. Kawada, H. Kawata, M. Tanaka, T. Arima, Y. Moritomo and Y. Tokura: Phys. Rev. Lett. **80** (1998) 1932; K. Nakamura, T. Arima, A. Nakazawa, Y. Wakabayashi and Y. Murakami: Phys. Rev. B **60** (1999) 2425.
3) Y. Moritomo, A. Nakamura, S. Mori, N. Yamamoto, K. Ohoyama and M. Ohashi: Phys. Rev. B**56** (1997) 14879; T. Akimoto, Y. Moritomo, K. Ohoyama, S. Okamoto, S. Ishihara, S. Maekawa and A. Nakamura: Phys. Rev. B**59** (1999) R14153.
4) A. Machida, Y. Moritomo, K. Ohoyama, S. Okamoto, S. Ishihara, S. Maekawa and A. Nakamura: Phys Rev. B **62** (2000) 80.
5) K. Ohoyama, T. Kanouchi, K. Nemoto, M. Ohashi, T. Kajitani and Y. Yamaguchi: Jpn. J. Appl. Phys. **37** (1998) 3319.
6) F. Izumi: "The Rietveld Method," ed. by R. A. Young, Oxford University Press, Oxford (1993), Chap.13; Y. -I. Kim and F. Izumi: J. Ceram. Soc. Jpn. **102** (1994) 401.